Hindawi Publishing Corporation
Abstract and Applied Analysis
Volume 2014, Article ID 513530, 8 pages
http://dx.doi.org/10.1155/2014/513530

Research Article

Feedforward and Feedback Vibration Control and Algorithm Design for Cable-Bridge Structure Nonlinear Systems

Yan-Jun Liang,[1] Shi-Liang Wu,[2] De-Xin Gao,[3] and Xiao-Rong Xue[1]

[1] *School of Computer and Information Engineering, Anyang Normal University, Anyang 455000, China*
[2] *School of Mathematics and Statistics, Anyang Normal University, Anyang 455000, China*
[3] *College of Automation and Electronic Engineering, Qingdao University of Science and Technology, Qingdao 266042, China*

Correspondence should be addressed to Yan-Jun Liang; myluck0404@126.com

Received 9 December 2013; Revised 15 February 2014; Accepted 20 February 2014; Published 23 March 2014

Academic Editor: Ryan Loxton

Technique of feedforward and feedback optimal vibration control and simulation for long-span cable-bridge coupled systems is developed. Buffeting loading systems of long-span cable-bridge structure are constructed by weighted amplitude wave superposition method. Nonlinear model of cable-bridge coupled vibration control system is established and the corresponding system of state space form is described. In order to reduce buffeting loading influence of the wind-induced vibration for the structure and improve the robust performance of the vibration control, based on semiactive vibration control devices and optimal control approach, a feedforward and feedback optimal vibration controller is designed, and an algorithm is presented for the vibration controller. Numerical simulation results are presented to illustrate the effectiveness of the proposed technique.

1. Introduction

Bridge plays an irreplaceable role in the transportation system and has an important value in politics, economy, culture, and military. Influenced by winds, vehicles, pedestrians, and seism loads, structural vibration of bridges is inevitable. Sustained and severe vibration of bridge structures not only shortens the service life of bridges but also reduces the security of traffic. Combined with extreme weather situations and geological disasters, accidents and dangerous cases happen frequently to bridge structures. Therefore, in order to decrease bridge vibration and to improve the reliability and safety of bridge structures, constructing vibration control systems has become an urgent problem to be solved.

Most of the studies on bridge structure focus on dynamic behavior [1–4], fatigue damage [4–6], and reliability analysis [7, 8]. Using frequency and time domain methods in [1], dynamic characteristics of a laboratory bridge model are determined by operational modal analysis. According to the actual project, the effects of bridge width and bridge deck pavement thickness on dynamic characteristics of hinge joint voided Slab bridge are researched in [2]. Considering wind, railway, and highway loadings in [3], dynamic stress analysis of long suspension bridges is presented. In [4], the dynamic properties of a decommissioned timber bridge are measured in the laboratory to observe the characteristics of the lowest few mode shapes as the support stiffness is varied to simulate deterioration of the pile supports, and an evaluation method is proposed to quantitatively assess the foundation competence of timber bridges. To avoid heavy interventions for strengthening of bridge deck slabs, in [5], an improved building material is used, fatigue tests for the determination of the fatigue behavior of beams reinforced by this building material are presented, and then a technique is developed to reduce the use costs as well as life cycle costs. The performance of an instrumented concrete bridge deck that has longitudinal cracks along with the entire length of the bridge is presented in [6], and the influence on their fatigue life is monitored. To analyze the reliability of Dongjiang Bridge, in [7], a new analysis method combined with advantages of some common reliability computing methods is put forward. The bridge is modeled as a single span simply supported Euler-Bernoulli beam and the vehicle is modeled as a single degree of freedom system in [8],

and they present a reliability analysis of a simply supported bridge deck subjected to random moving and seismic loads. The previous studies are mostly about the vibration response, monitor, and analysis [9–11], but few studies are about vibration control for bridge structure, and the result about optimal control problems [12–15] for nonlinear systems of the bridge structure vibration control is rare.

The remainder of this paper is structured as follows. In Section 2, first, employing weighted amplitude wave superposition method and buffeting loading forces on long-span cable-bridge structure are established. Then, mechanical model and dynamical system of the long-span cable bridge are constructed. In Section 3, optimal vibration problem of cable-bridge systems is presented. In Section 4, first, in order to use successive approximation approach (SAA), two lemmas are introduced. Then, feedforward and feedback optimal vibration controller and algorithm are designed for the long-span cable-bridge system. In Section 5, numerical experiments are presented. Finally, in Section 6 some conclusions are drawn.

2. Cable-Bridge Structure Nonlinear Control System

2.1. Buffeting Loading. As the span of the bridge extends, the stiffness of the bridge structure reduces, and the bridge has much more characteristics of the flexible structure. Therefore, the influence of the wind loading on the bridge structure cannot be neglected in engineering, and many scholars turn their attention to the influence of the wind-induced vibration on the structure. Bridge buffeting is a sort of random vibration of the bridge structure influenced by the fluctuating wind. Fluctuating wind field induced by natural wind can be described by ergodic and stationary Gauss random process and can be regarded as a single variable four-dimensional random field in mathematics.

We employ weighted amplitude wave superposition method to describe buffeting loading forces on long-span cable-bridge structures. According to weighted amplitude wave superposition method, buffeting loading forces on long-span cable-bridge structure can be simulated by superposition of weighted amplitude waves. The buffeting force of the jth composition wave on long-span cable-bridge structure is as follows:

$$\overline{p}_j = A_j \sin\left(\omega_j t + \varphi_j\right), \quad j = 1, 2, \ldots, r, \tag{1}$$

in which A_j and ω_j are, respectively, the amplitude and frequency of the jth wave component and φ_j is the random phase angles uniformly distributed in $0 \le \varphi_j < 2\pi$. Let $\widetilde{p}(t) = [\overline{p}_1, \overline{p}_2, \ldots, \overline{p}_r]^T$; we have

$$\begin{aligned} \ddot{\overline{p}}_j &= -\omega_j^2 \overline{p}_j, \quad j = 1, 2, \ldots, r, \\ \ddot{\widetilde{p}}(t) &= -\operatorname{diag}\left\{\omega_1{}^2, \omega_2{}^2, \ldots, \omega_r{}^2\right\} \widetilde{p}(t) \\ &= -\overline{\Omega}^2 \widetilde{p}(t), \end{aligned} \tag{2}$$

in which $\overline{\Omega} = \operatorname{diag}\{\omega_1, \omega_2, \ldots, \omega_r\}$. Let $w(t) = \left[\widetilde{p}(t) \;\; \dot{\widetilde{p}}(t)\right]^T$; then

$$\begin{aligned} \dot{w}(t) &= \begin{bmatrix} 0 & I_r \\ -\overline{\Omega}^2 & 0 \end{bmatrix} w(t) = \overline{G} w(t), \\ \widetilde{p}(t) &= \begin{bmatrix} I_r & 0 \end{bmatrix} w(t), \\ p(t) &= [1, \ldots, 1]\, \widetilde{p}(t) \\ &= \left[\underbrace{1, \ldots, 1}_{r}, \underbrace{0, \ldots, 0}_{r}\right] w(t) = \overline{F} w(t), \end{aligned} \tag{3}$$

where $\overline{F} = [\underbrace{1, \ldots, 1}_{r}, \underbrace{0, \ldots, 0}_{r}]$, $\overline{G} = \begin{bmatrix} 0 & I_r \\ -\overline{\Omega}^2 & 0 \end{bmatrix}$, I_r is the r-order unit matrix, and $0 \in R^{r \times r}$ is the zero matrix.

So, the total buffeting loading force acting on the bridge structure can be generated by the exosystem:

$$\begin{aligned} \dot{w}(t) &= \overline{G} w(t), \\ p(t) &= \overline{F} w(t). \end{aligned} \tag{4}$$

2.2. Mechanical Model and Dynamical System. Considering cable-bridge structures with semiactive tune mass damper devices, the deck is simplified as the lumped mass influenced by the cable end and is denoted by the parameter M. And the stiffness and damping of the deck are represented by C and K, respectively. The cable-bridge coupled vibration induced by the buffeting loading is decomposed into the motion along the axial direction and the motion perpendicular to the cable axis. The problem of the axial direction motion is studied in this paper. The mechanical model of the cable and deck is shown in Figure 1.

In order to simplify the problem and reflect the essence of the vibration control for the cable-bridge structure, we make some fundamental assumptions as follows:

(1) the flexural stiffness, torsional stiffness, and shear stiffness are disregarded;

(2) the gravity sag curve is considered as a parabola;

(3) the constitutive relation of the deformation for the cable satisfies Hooke's law and is uniform for each point;

(4) the effect of the tower vibration on the cable is disregarded.

Generally, the fundamental mode is in the dominant position; therefore we consider the first mode as the main object to study the cable-bridge coupled vibration control problem. The dynamical system of the cable-bridge coupled vibration induced by the buffeting loading is as follows:

$$\begin{aligned} &\ddot{W}(t) + \left(\omega_1^2 + a_3 Y(t)\right) W(t) + a_1 W^3(t) \\ &\qquad + a_2 W^2(t) + a_4 Y(t) = 0, \\ &u(t) + p(t) = \ddot{Y}(t) + 2\omega_2 \xi \dot{Y}(t) \\ &\qquad + \omega_2^2 Y(t) + a_5 W(t) + a_6 W^2(t), \end{aligned} \tag{5}$$

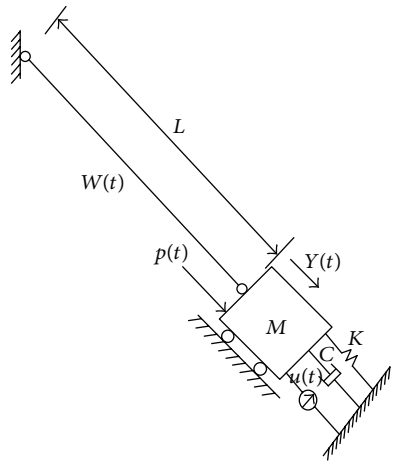

Figure 1: The mechanical model of cable and deck.

in which $W(t)$ is cable displacement from the equilibrium position; $Y(t)$ is the displacement of the cable end, namely, the deck displacement along the axial direction of the cable; $u(t)$ is control input variable; ω_1 and ω_2 are the intrinsic frequencies of the cable and deck, respectively; ξ is the damping ratio of the deck; a_i $(i = 1, 2, \ldots, 6)$ are parameters determined by the factors such as the mass per unit length and the dip angle of the cable and the regular function of the deck vibration mode.

Choose state variables and state vector for the cable-bridge coupled vibration control system (5) as follows:

$$\begin{aligned} x_1(t) &= W(t), \qquad x_2(t) = \dot{W}(t), \\ x_3(t) &= Y(t), \qquad x_4(t) = \dot{Y}(t), \\ x(t) &= \left[x_1(t), x_2(t), x_3(t), x_4(t)\right]^T, \end{aligned} \tag{6}$$

and the system (5) is rewritten in the state-space representation:

$$\begin{aligned} \dot{x}(t) &= Ax(t) + Bu(t) + f(x) + Dp(t), \\ x(0) &= x_0, \end{aligned} \tag{7}$$

where $p(t)$ is external input disturbance, namely, buffeting loading force, and

$$A = \begin{bmatrix} 0 & 1 & 0 & 0 \\ -\omega_1^2 & 0 & -a_4 & 0 \\ 0 & 0 & 0 & 1 \\ -a_5 & 0 & -\omega_2^2 & -2\omega_2\xi \end{bmatrix},$$

$$B = \begin{bmatrix} 0 \\ 0 \\ 0 \\ 1 \end{bmatrix}, \qquad D = \begin{bmatrix} 0 \\ 0 \\ 0 \\ 1 \end{bmatrix},$$

$$f(x) = \left[0 \quad -a_1 x_1^3(t) - a_2 x_1^2(t) - a_3 x_3(t) x_1(t) \quad 0 \quad -a_6 x_1^2(t)\right]^T. \tag{8}$$

3. Optimal Vibration Control Problem of the Long-Span Cable-Bridge System

In order to study optimal vibration control problem for long-span cable-bridge, we choose an average performance index for system (7) as follows:

$$J = \lim_{T \to \infty} \frac{1}{T} \int_0^T \left[x^T(t) Q x(t) + R u^2(t)\right] dt, \tag{9}$$

where $Q \in \mathbb{R}^{4\times4}$ are positive semidefinite matrices and $R \in \mathbb{R}$ is a positive definite matrix.

The objective of this paper is to find a control law $u^*(t)$ for system (7) and make the value of the performance index (9) a minimum.

Applying the maximum principle to the optimal control problem in (7) and (9), the optimal control law is described by

$$u^*(t) = -R^{-1} B^T \lambda(t), \tag{10}$$

where $\lambda(t)$ is the solution to the following nonlinear two-point boundary value (TPBV) problem:

$$\begin{aligned} -\dot{\lambda}(t) &= Qx(t) + A^T \lambda(t) + {f_x}^T(x)\lambda(t), \\ \dot{x}(t) &= Ax(t) - S\lambda(t) + f(x) + Dp(t), \\ x(0) &= x_0, \\ \lambda(\infty) &= 0, \end{aligned} \tag{11}$$

where $S = BR^{-1}B^T$ and ${f_x}^T(x) = \partial f^T(x)/\partial x$ is the Jacobian matrix of $f(x)$ with respect to vector x.

Unfortunately, for the nonlinear TPBV problem in (11), with the exception of the simplest cases, there is no analytic solution. Therefore, we try to find the numerical solution to such problem. The main purpose of this paper is to develop SAA [15] in order to find the feedforward and feedback optimal control law for the system described by (7) with average performance index (9). In this approach, the optimal control law is composed of exact linear term and the compensation of the nonlinear term. The compensation of the nonlinear term is the limit of the costate vector iteration sequence. The original optimal control law is approached by the process of solving the iteration sequence, instead of solving the nonlinear TPBV problem.

4. Optimal Vibration Control Law Design

Consider the nonlinear system

$$\begin{aligned} \dot{z}(t) &= G(t) z(t) + h(z(t), t) + Fv(t), \\ z(t_1) &= \eta, \end{aligned} \tag{12}$$

where $z \in \mathbb{R}^n$ is the state vector, $v \in \mathbb{R}^m$ is the input vector, $h : \mathbb{R}^n \times \mathbb{R}_+ \to U$, $h(0, t) \equiv 0$, $\overline{G} : \mathbb{R}_+ \to \mathbb{R}^{n\times n}$, $F \in \mathbb{R}^{n\times m}$, and η is the initial state vector (for $t_1 = t_0$) or the terminal state vector (for $t_1 = t_f$). Assume that h satisfies the Lipschitz conditions on $\mathbb{R}^n \times \mathbb{R}_+$.

In order to use the SAA, we introduce two lemmas [16].

Lemma 1. *Define the vector function sequence* $\{z^{(k)}(t)\}$ *as*

$$\begin{aligned} z^{(0)}(t) &= \Phi(t,t_0)\eta + \int_{t_0}^{t} \Phi(t,r) F v(r)\, dr, \\ z^{(k)}(t) &= \Phi(t,t_0)\eta \\ &\quad + \int_{t_0}^{t} \Phi(t,r)\left[h\left(z^{(k-1)}(r), r\right) + F v(r)\right] dr, \\ &\qquad k = 1,2,\ldots, \quad t \in \mathbb{R}_T, \end{aligned} \tag{13}$$

where $\Phi(t,t_0)$ *is the state transition matrix corresponding to* $G(t)$*; then the sequence* $\{z^{(k)}(t)\}$ *uniformly converges to the solution of* (12) *for* $t_1 = t_0$.

Lemma 2. *Define the vector function sequence* $\{z^{(k)}(t)\}$ *as*

$$\begin{aligned} z^{(0)}(t) &= \Phi\left(t,t_f\right)\eta + \int_{t_f}^{t} \Phi(t,r) F v(r)\, dr, \\ z^{(k)}(t) &= \Phi\left(t,t_f\right)\eta \\ &\quad + \int_{t_f}^{t} \Phi(t,r)\left[h\left(z^{(k-1)}(r), r\right) + F v(r)\right] dr, \\ &\qquad k = 1,2,\ldots, \quad t \in \mathbb{R}_T. \end{aligned} \tag{14}$$

Then the sequence $\{z^{(k)}(t)\}$ *converges uniformly to the solution of system* (12) *as* $t_1 = t_f$.

4.1. Feedforward and Feedback Optimal Controller and Algorithm Design. Then, we design vibration controller for system (7). The optimal control law can be presented in the following theorem.

Theorem 3. *Consider the optimal control problem described by system* (7) *with performance index* (9)*, the feedforward and feedback optimal control law* $u^*(t)$ *exists and is unique. Its form is as follows:*

$$\begin{aligned} u^*(t) = -R^{-1}B^T \Big[& P_1 x(t) + P_2 p(t) \\ & + P_3 p_\omega(t) + \lim_{k\to\infty} g^{(k)}(t) \Big], \end{aligned} \tag{15}$$

where P_1 *is the unique positive definite solution of the following Riccati matrix equation:*

$$A^T P_1 + P_1 A - P_1 S P_1 + Q = 0. \tag{16}$$

P_2 *and* P_3 *are the unique solutions of the following Sylvester matrix equations:*

$$\begin{aligned} \left(A^T - P_1 S\right)^2 P_2 \overline{F} + P_2 \overline{F} \Omega^2 &= -\left(A^T - P_1 S\right) P_1 D \overline{F}, \\ \left(A^T - P_1 S\right)^2 P_3 + P_3 \Omega^2 &= P_1 D. \end{aligned} \tag{17}$$

The kth adjoint vector is found from the following adjoint vector sequences:

$$\begin{aligned} g^{(0)}(t) &= \int_t^\infty \Phi^T(r-t)\, {f_x}^T(0)\left[P_2 p(r) + P_3 p_\omega(r)\right] dr, \\ g^{(k)}(t) &= \int_t^\infty \Phi^T(r-t)\Big\{P_1 f\left(x^{(k-1)}(r)\right) + {f_x}^T\left(x^{(k-1)}(r)\right) \\ &\qquad \times \Big[P_1 x^{(k-1)}(r) + P_2 p(r) \\ &\qquad + P_3 p_\omega(r) + g^{(k-1)}(r)\Big]\Big\} dr, \\ &\qquad k = 1,2,\ldots, \end{aligned} \tag{18}$$

and the kth state vectors $x^{(k)}(t)$ *satisfy the following state vector sequences:*

$$\begin{aligned} x^{(0)}(t) &= \Phi(t)\, x_0 \\ &\quad + \int_0^t \Phi(r-t)\Big[\left(D - SP_2\right) p(r) \\ &\qquad - SP_3 p_\omega(r) - S g^{(0)}(r)\Big] dr, \\ x^{(k)}(t) &= \Phi(t)\, x_0 \\ &\quad + \int_0^t \Phi(r-t)\Big[\left(D - SP_2\right) p(r) - SP_3 p_\omega(r) \\ &\qquad - S g^{(k)}(r) + f\left(x^{(k-1)}(r)\right)\Big] dr, \\ &\qquad k = 1,2,\ldots, \end{aligned} \tag{19}$$

$$\begin{aligned} \Phi(t) &= e^{(A - SP_1)t}, \\ \Omega &= \operatorname{diag}\left\{\overline{\Omega}, \overline{\Omega}\right\}, \\ p_\omega(t) &= \dot{p}(t) = \overline{F}\,\overline{G} w(t). \end{aligned} \tag{20}$$

Proof. To use the SAA to solve nonlinear TPBV problem (11), we separate the linear part in nonlinear TPBV problem (11); let

$$\lambda(t) = P_1 x(t) + P_2 p(t) + P_3 \dot{p}(t) + g(t), \tag{21}$$

where $g(t)$ is an adjoint vector introduced to compensate for the effect of the nonlinear term in system (7).

Substituting the first equation of (7) and (10) into the derivative of (21), we get

$$\begin{aligned} \dot{\lambda}(t) &= P_1 \dot{x}(t) + P_2 \dot{p}(t) + P_3 \ddot{p}(t) + \dot{g}(t) \\ &= \left(P_1 A - P_1 S P_1\right) x(t) + \left(P_1 D - P_1 S P_2\right) p(t) \\ &\quad + \left(P_2 - P_1 S P_3\right) \dot{p}(t) + P_3 \ddot{p}(t) \\ &\quad - P_1 S g(t) + P_1 f(x) + \dot{g}(t). \end{aligned} \tag{22}$$

Note that

$$p_\omega(t) = \dot{p}(t),$$
$$\ddot{p}(t) = \overline{F}G^2 w(t) = -\overline{F}\Omega^2 w(t). \tag{23}$$

From (11) and (21), we obtain

$$\dot{\lambda}(t) = -\left(Q + A^T P_1\right) x(t) - A^T P_2 p(t) - A^T P_3 p_\omega(t) - A^T g(t) - f_x^T(x)\lambda(t). \tag{24}$$

Substituting (23) into (22) and comparing the coefficients of (22) and (24), we obtain matrix equations:

$$A^T P_1 + P_1 A - P_1 S P_1 + Q = 0,$$
$$A^T P_2 \overline{F} + P_1 D\overline{F} - P_3 \overline{F}\Omega^2 - P_1 S P_2 \overline{F} = 0, \tag{25}$$
$$A^T P_3 + P_2 - P_1 S P_3 = 0,$$

and the adjoint vector differential equations:

$$\dot{g}(t) = -(A - SP_1)^T g(t) - P_1 f(x) - f_x^T(x)\lambda(t), \quad g(\infty) = 0. \tag{26}$$

From the matrix equations in (25), we obtain

$$A^T P_1 + P_1 A - P_1 S P_1 + Q = 0,$$
$$\left(A^T - P_1 S\right)^2 P_2 \overline{F} + P_2 \overline{F}\Omega^2 = -\left(A^T - P_1 S\right) P_1 D\overline{F}, \tag{27}$$
$$\left(A^T - P_1 S\right)^2 P_3 + P_3 \Omega^2 = P_1 D.$$

Substituting (21) into the second equation of TPBV problem (11), we have

$$\dot{x}(t) = \left(A - SP_1\right) x(t) + \left(D - SP_2\right) p(t) - SP_3 p_\omega(t) - Sg(t) + f(x), \quad x(t_0) = x_0. \tag{28}$$

In order to obtain the solution of TPBV problem (11) from the SAA, according to (28) and (26), we construct the following state equation sequences:

$$\dot{x}^{(0)}(t) = \left(A - SP_1\right) x^{(0)}(t) + \left(D - SP_2\right) p(t) - SP_3 p_\omega(t) - Sg^{(0)}(t), \quad x^{(0)}(t_0) = x_0,$$
$$\dot{x}^{(k)}(t) = \left(A - SP_1\right) x^{(k)}(t) + \left(D - SP_2\right) p(t) - SP_3 p_\omega(t) - Sg^{(k)}(t) + f\left(x^{(k-1)}\right), \quad x^{(k)}(t_0) = x_0, \quad k = 1, 2, \ldots, \tag{29}$$

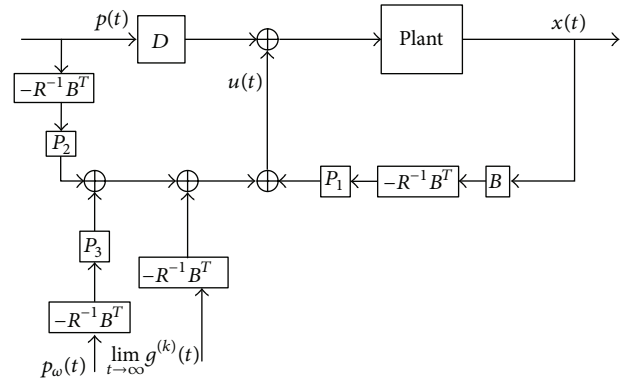

Figure 2: Control block diagram of the system.

and the adjoint vector differential equation sequences:

$$\dot{g}^{(0)}(t) = -(A - SP_1)^T g^{(0)}(t) - f_x{}^T(0)\left[P_2 p(t) + P_3 p_\omega(t)\right], \quad \lim_{T\to\infty} g^{(0)}(T) = 0,$$
$$\dot{g}^{(k)}(t) = -(A - SP_1)^T g^{(k)}(t) - P_1 f\left(x^{(k-1)}(t)\right) - f_x{}^T\left(x^{(k-1)}(t)\right)\lambda^{(k-1)}(t), \quad \lim_{T\to\infty} g^{(0)}(T) = 0, \quad k = 1, 2, \ldots, \tag{30}$$

where

$$\lambda^{(k)}(t) = P_1 x^{(k)}(t) + P_2 p(t) + P_3 p_\omega(t) + g^{(k)}(t), \quad k = 1, 2, \ldots. \tag{31}$$

According to Lemmas 1 and 2, the adjoint vector sequence in (18) and the state vector sequences in (19) uniformly converge to the solution of (26) and (28), respectively.

Correspondingly, the control sequence is given in the following form:

$$u^{(k)}(t) = -R^{-1}B^T\lambda^{(k)}(t) = -R^{-1}B^T\left[P_1 x^{(k)}(t) + P_2 p(t) + P_3 p_\omega(t) + g^{(k)}(t)\right]. \tag{32}$$

When $k \to \infty$, we obtain the feedforward and feedback optimal control law $u^*(t)$ in (15).

From (15), we can see that the feedforward and feedback optimal control law $u^*(t)$ is composed of the state feedback term, the disturbance and its derivative, and the compensation of the nonlinear term of the cable-bridge vibration control system. In order to explain the work of the control law, the control block diagram of the system is drawn simply in Figure 2. □

Remark 4. In fact, it is impossible to calculate feedforward and feedback optimal control law in (15). We can find the

feedforward and feedback optimal control law by replacing ∞ with N in (15):

$$u_N(t) = -R^{-1}B^T\left[P_1 x(t) + P_2 p(t) + P_3 p_\omega(t) + g^{(N)}(t)\right]. \quad (33)$$

In order to implement the feedforward and feedback control law described in Theorem 3, we design an algorithm in the following.

Algorithm 5. Consider the following.

Step 1. Calculate the matrices P_1, P_2, and P_3 from the matrix equations (16) and (17).

Step 2. Establish the buffeting loading force $p(t)$ by the model (4) and relevant data from (23).

Step 3. Choose an allowable error σ.

Step 4. Calculate $g^{(0)}(t)$ and $x^{(0)}(t)$ by the first equations of (18) and (19), respectively, and let $i = 1$.

Step 5. Calculate $g^{(i)}(t)$ and $x^{(i)}(t)$ by the second equations of (18) and (19), respectively.

Step 6. Calculate the ith feedforward and feedback optimal controller $u^{(i)}(t)$ by (32).

Step 7. Calculate $J^{(i)}$:

$$J^{(i)} = \lim_{T\to\infty}\frac{1}{T}\int_0^T\left[x^{(i)^T}(t)\,Qx^{(i)}(t) + Ru^{(i)^2}(t)\right]dt. \quad (34)$$

If $|J^{(j)} - J^{(j-1)}|/J^{(j)} \le \sigma$, $j = i, i-1, i-2, i-3$, and $i \ge 4$, stop calculating, and N can be chosen from $[i-3, i]$. The Nth order feedforward and feedback optimal controller $u_N(t)$ is obtained by (33); else let $i = i + 1$ and go to Step 5.

5. Numerical Simulations

In this section, we apply the proposed feedforward and feedback optimal vibration controller to a road suspension cable-bridge. The cable-bridge with three towers located in Yangtze River, whose span arrangement is 360 m + 1080 m + 1080 m + 360 m = 2880 m, whose stiffening beam of 3.5 m height and 38.5 m width with a tuyere consisting of a top and a bottom inclined plates is closed flat steel box beam, whose cable bent towers are 178.3 m high, whose two main cables crosswise space between is 35.8 m, whose main part of tower is filled by concrete and is H model, and whose middle tower is supported by expanded triangle. The values of system (7) and performance index (9) are as follows: $\omega_1 = 0.470$ Hz, $\omega_2 = 0.793$ Hz, $\xi = 0.02$, $a_i = 1.15$ $(i = 1, 2, \ldots, 6)$, $Q = I$, and $R = 1$.

Employing Matlab software, numerical experiments are carried out for the proposed optimal vibration controller. Figure 3 shows the buffeting loading force curve.

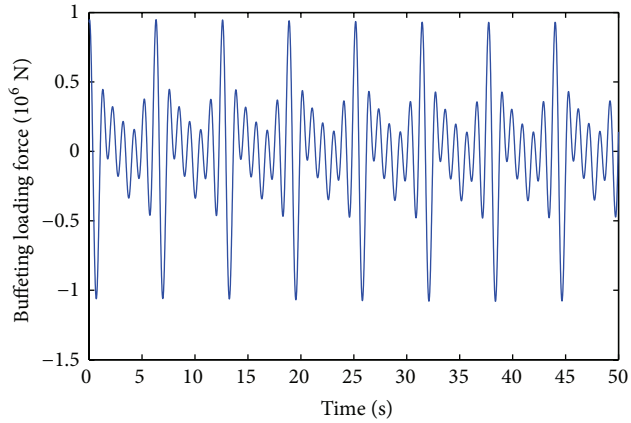

Figure 3: Buffeting loading force curve.

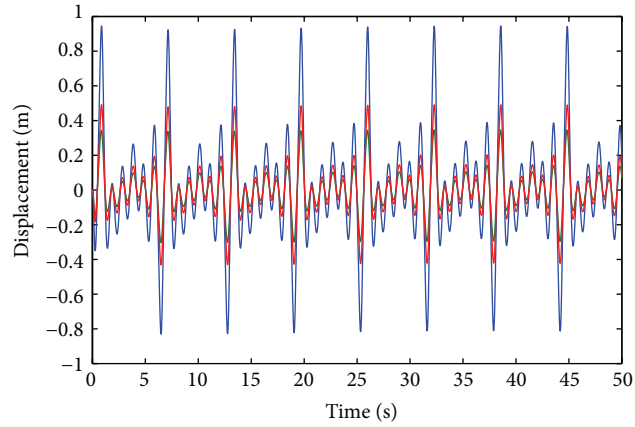

Figure 4: Displacement curves.

The main purpose of vibration control of long-span cable-bridge is to reduce the deck displacement which indicates the limit of the deck motion and to reduce the deck velocity which ensures the road holding ability for vehicles and pedestrians. So, to evaluate effectiveness of the proposed control strategy, the deck displacement and velocity are considered. Then, the corresponding curves of open loop system, feedback optimal control system, and the system controlled by the proposed optimal vibration controller are compared and shown in Figures 4 and 5. Then, in Figure 6, the control forces of the feedback controller represented by the red line and proposed controller denoted by the green line are shown.

The curves of displacement are shown in Figure 4 and velocities are in Figure 5, in which blue lines represent the open loop results of the deck of long-span bridge systems, red lines denote the results controlled by feedback optimal controller, and green lines describe the results of the long-span bridge systems controlled by the proposed control strategy. It can be seen from Figures 4 and 5 that the proposed optimal controller is efficient, real-time, and robust in reducing displacement and velocity of the deck, thereby ensures safety of the long-span bridge, and enhances passing vehicle

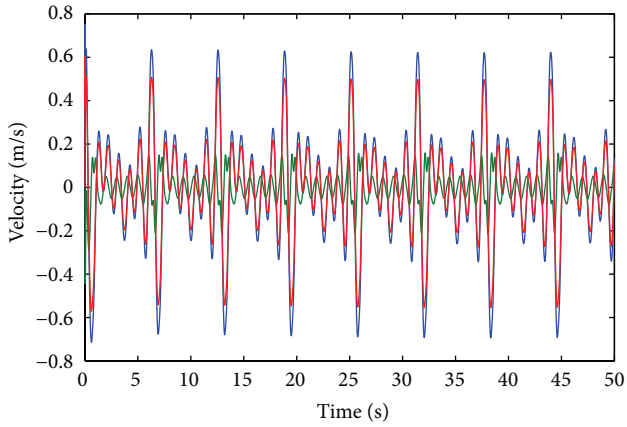

Figure 5: Velocity curves.

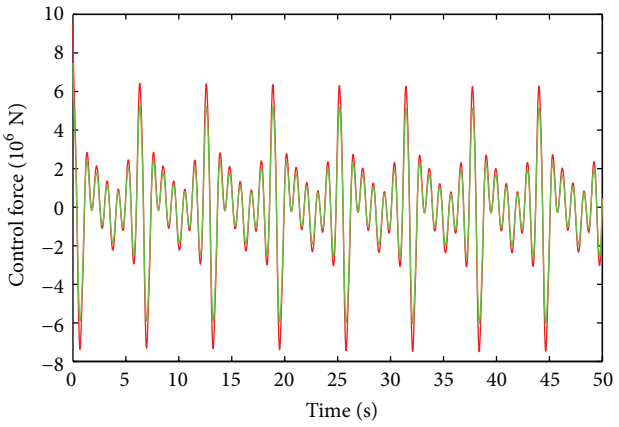

Figure 6: Control force curves.

ride comfort. Moreover, in Figure 6, it is demonstrated that it needs less control forces than feedback optimal vibration control and therefore it needs less energy. In Figure 5, the system controlled by the proposed controller (green line) responds much quicker than that controlled by feedback controller (red line), but, as it is shown in Figure 6, the output of two controllers is synchronous in terms of changing time; this is the trait and merit of optimal control. In fact, we can change the weighting matrix Q and the weighting coefficient R to balance the control effect and control energy.

6. Conclusions

The effect of the wind-induced vibration on the long-span cable-bridge structure cannot be neglected in construction phase or in operation stage. The influence of buffeting loading and nonlinear factor for long-span cable-bridge structures is considered in this paper. Based on the semiactive vibration control devices, optimal vibration controller and control algorithm are designed for the long-span cable-bridge. Numerical simulation results show that the proposed strategy is efficient, real-time, and robust in reducing the vibration induced by buffeting loading.

Conflict of Interests

The authors declare that there is no conflict of interests regarding the publication of this paper.

Acknowledgments

This research was supported by Natural Science Foundation of China (nos. 11301009, U1204402, and 61374003) and Natural Science Foundations of Henan Province Education Department (nos. 12A120001, 13A520018, 14B520018, and 13A110022).

References

[1] A. C. Altunisik, A. Bayraktar, and B. Sevim, "Operational modal analysis of a scaled bridge model using EFDD and SSI methods," *Indian Journal of Engineering and Materials Sciences*, vol. 19, no. 5, pp. 320–330, 2012.

[2] Y. Zhou and Z. Chen, "Dynamic analysis of hinge joint voided slab wide bridge," in *Proceedings of the International Conference on Electric Technology and Civil Engineering (ICETCE '11)*, pp. 246–249, April 2011.

[3] Z. W. Chen, Y. L. Xu, Q. Li, and D. J. Wu, "Dynamic stress analysis of long suspension bridges under wind, railway, and highway loadings," *Journal of Bridge Engineering*, vol. 16, no. 3, pp. 383–391, 2011.

[4] C. J. Beauregard, B. F. Sparling, and L. D. Wegner, "Vibration-based damage detection for support softening under a simply supported timber bridge," in *Proceedings of the Annual Conference of the Canadian Society for Civil Engineering (CSCE '10)*, pp. 1214–1223, June 2010.

[5] T. Makita and E. Brhwiler, "Fatigue behaviour of bridge deck slab elements strengthened with reinforced UHPFRC," in *Proceedings of the 6th International Conference on Bridge Maintenance, Safety and Management*, pp. 1974–1980, 2012.

[6] G. W. William, S. N. Shoukry, and M. Y. Riad, "Monitoring of field performance of longitudinally cracked concrete bridge deck," in *Proceedings of the 6th International Conference on Bridge Maintenance, Safety and Management*, pp. 3984–3991, 2012.

[7] J. Liu and Y.-J. Liu, "Reliability analysis of continuous steel truss bridge stiffened with rigid cables based on stochastic finite element method," in *Proceedings of the 1st International Conference on Advances in Civil Infrastructure Engineering*, pp. 1060–1066, 2012.

[8] D. Sen, B. Bhattacharya, and C. S. Manohar, "Reliability of bridge deck subject to random vehicular and seismic loads through subset simulation," in *Proceedings of the 6th International Conference on Bridge Maintenance, Safety and Management*, pp. 668–675, 2012.

[9] Y. Shi, S. Fang, Q. Tian, and W. Chen, "Spatial numerical analysis method of coupled vibration between whole vehicle model and curved bridge caused by bridge deck roughness," *Advanced Materials Research*, vol. 446–449, pp. 1270–1276, 2012.

[10] W. Han and A. Chen, "Three-dimensional coupling vibration of wind-vehicle-bridge systems," *China Civil Engineering Journal*, vol. 40, no. 9, pp. 53–58, 2007 (Chinese).

[11] C. Schulz and N. Gallino, "Condition assessment and dynamic system identification of a historic suspension footbridge," *Structural Control and Health Monitoring*, vol. 15, no. 3, pp. 369–388, 2008.

[12] Q. Lin, R. Loxton, and K. L. Teo, "The control parameterization method for nonlinear optimal control: a survey," *Journal of Industrial and Management Optimization*, vol. 10, no. 1, pp. 275–309, 2014.

[13] Q. Lin, R. Loxton, K. L. Teo, and Y. H. Wu, "Optimal control computation for nonlinear systems with state-dependent stopping criteria," *Automatica*, vol. 48, no. 9, pp. 2116–2129, 2012.

[14] C. Jiang, Q. Lin, C. Yu, K. L. Teo, and G.-R. Duan, "An exact penalty method for free terminal time optimal control problem with continuous inequality constraints," *Journal of Optimization Theory and Applications*, vol. 154, no. 1, pp. 30–53, 2012.

[15] G.-Y. Tang, "Suboptimal control for nonlinear systems: a successive approximation approach," *Systems & Control Letters*, vol. 54, no. 5, pp. 429–434, 2005.

[16] G.-Y. Tang and D.-X. Gao, "Approximation design of optimal controllers for nonlinear systems with sinusoidal disturbances," *Nonlinear Analysis. Theory, Methods & Applications*, vol. 66, no. 2, pp. 403–414, 2007.